International Journal of Fatigue 147 (2021) 106153

Contents lists available at ScienceDirect

International Journal of Fatigue

journal homepage: www.elsevier.com/locate/ijfatigue

Parameter estimation of a high-cycle fatigue model combining the Ottosen-Stenström-Ristinmaa approach and Lemaitre-Chaboche damage rule

Osmo Kaleva [a], Heikki Orelma [a,*], Dmitriy Petukhov [b]

[a] Tampere University, Mathematics, P.O. Box 692, 33014 Tampere, Finland
[b] Institute of Continuous Media Mechanics UB RAS, 1 Akademika Koroleva Str., Perm 614013, Russian Federation

ARTICLE INFO

Keywords:
High-cycle fatigue
Damage evolution
Continuum mechanics-based model
Lemaitre-Chaboche damage rule

ABSTRACT

This paper deals with the continuum approach to the high-cycle fatigue model introduced by Ottosen et al. equipped with the damage rule of Lemaitre and Chaboche. The main result is that model parameters K and γ are not identifiable based on lifetime data. However, with observations from a fatigue development profile, it is possible to estimate also the γ-parameter. Moreover, the model gives the same lifetime for all $\gamma \geqslant 0$. These results are elucidated with examples.

1. Introduction

Fatigue of materials under variable loading histories is caused by a complicated physical process, which is characterized among other things by initiation, coalescence and the growth of cracks. Lemaitre and Chaboche [8] as well as Suresh [26] provide a comprehensive discussion on this topic.

Since the days of Wöhler, problems related to the development of material fatigue damage have been studied. In the past decades, the effects of various mechanical, micro structural and environmental factors on cyclic deformation as well as on crack initiation and growth in a vast spectrum of engineering materials have been the topics of considerable research. In addition, it is experimentally observed that some physical processes causing fatigue failure behave differently in the high-cycle fatigue domain and very-high-cycle fatigue domain [11,15,21].

Fatigue studies are important, since frequently a failure of mechanical components is caused by fatigue. A design engineer needs information on the fatigue durability of a material. In addition to the lifetime, it is important to know for example how much is, say 80%, of the lifetime. For an answer, an understanding of the damage development is necessary. In this paper, we use a fatigue model as introduced by Ottosen et al. [14], the OSR model for short. Recent developments in this model are discussed for instance in [10,13,27].

Over the years, several fatigue damage models have been proposed. The earliest assumption was the linear accumulation of failure by Miner [12]. Modern measurement techniques show that the linear model is too rudimentary. Damage usually develops slowly at first and only later on starts to accelerate. Hence, it is natural to look for nonlinear damage models. Many of these models get their motivation and inspiration from the works of Lemaitre and Chaboche [8]. A nice survey of the existing and most used models and historical remarks can be found for example in the works of Aeran et al. [1,2]. The main reason for the interest in new models is due to the development of measurement techniques. These are based, to the best of the authors' knowledge, on the yield stress [16,17], the ductility [4,23], the dissipated energy [24], the modulus of elasticity [19] and the hardness change during fatigue [18]. In this paper we consider a damage rule (7), as defined in Section 3. It is the damage rule of Lemaitre–Chaboche type, and it is used with the evolution equation-based continuum model, see *e.g.* [7]. The adoption of this damage rule introduces an extra parameter to the model. This parameter, denoted as γ, makes the damage evolution profile explicit. It is well known, cf. [14], that parameters of the OSR model can be estimated from lifetime measurements of a material. This, however, does not hold true for the γ-parameter. For the estimation of γ, additional measurements from the damage accumulation profile are needed. Detailed algorithms and methods for estimation, as well as some illustrative examples, are given.

2. Damage evolution-based continuum model

In this section, we briefly recall the basic ideas of evolution equation-

* Corresponding author.
E-mail addresses: osmo.kaleva@gmail.com (O. Kaleva), heikki.orelma@tuni.fi (H. Orelma), petuhovds@mail.ru (D. Petukhov).

https://doi.org/10.1016/j.ijfatigue.2021.106153
Received 23 September 2020; Received in revised form 11 January 2021; Accepted 11 January 2021
Available online 14 February 2021
0142-1123/© 2021 The Authors. Published by Elsevier Ltd. This is an open access article under the CC BY license (http://creativecommons.org/licenses/by/4.0/).

based fatigue as introduced in [14]. The fundamental idea is to define the so-called endurance surface

$$\beta(\boldsymbol{\sigma},\boldsymbol{\alpha}) = 0 \tag{1}$$

in stress space. A symmetric tensor $\boldsymbol{\alpha}$ is called a backstress, in the spirit of plasticity theory, and intuitively it presents the centre of the endurance surface. A tensor $\boldsymbol{\sigma}$ is a stress history. The *fundamental postulate* of the model is that the endurance surface and the damage develops simultaneously when the deviatoric part of $\boldsymbol{\sigma}$ is located outside the endurance surface and moves away from it. More precisely, the surface moves when the conditions $\beta(\boldsymbol{\sigma},\boldsymbol{\alpha})\geqslant 0$ and $\dot{\beta}(\boldsymbol{\sigma},\boldsymbol{\alpha})\geqslant 0$ are fulfilled.

As in [14], the function of the form

$$\beta\left(\boldsymbol{\sigma},\boldsymbol{\alpha}\right) = \frac{1}{\sigma_{-1}}\left(\overline{\sigma} + AI_1 - \sigma_{-1}\right), \tag{2}$$

is used, where σ_{-1} and A are positive material parameters and $I_1 = \mathrm{tr}(\boldsymbol{\sigma})$ is the first stress invariant of $\boldsymbol{\sigma}$. The so-called effective stress is defined by

$$\overline{\sigma} = \sqrt{\frac{3}{2}}\left\|\boldsymbol{\sigma} - \frac{\mathrm{tr}(\boldsymbol{\sigma})}{3}\mathbf{I} - \boldsymbol{\alpha}\right\|_{\mathrm{F}}, \tag{3}$$

where $\mathbf{I}$ is the identity matrix and the norm is just the Frobenius norm. Recall that for symmetric matrices, the Frobenius norm can be written as $\|A\|_{\mathrm{F}}^2 = \mathrm{tr}(A^2)$. The variable $\boldsymbol{\alpha}$ denotes the centre of the endurance surface, and it is governed by the evolution equation

$$\dot{\boldsymbol{\alpha}} = \begin{cases} C\left(\boldsymbol{\sigma} - \frac{\mathrm{tr}(\boldsymbol{\sigma})}{3}\mathbf{I} - \boldsymbol{\alpha}\right)\dot{\beta}, & \text{if } \beta\geqslant 0,\ \dot{\beta}\geqslant 0, \\ 0, & \text{otherwise}, \end{cases} \tag{4}$$

where C is a positive material parameter. Observe that the centre $\boldsymbol{\alpha}$ moves only when the stress state moves away from the endurance surface outside of it.

As mentioned above, due to the fundamental postulate, the damage increases when the centre $\boldsymbol{\alpha}$ moves. The damage development D is modelled by the initial value problem

$$\dot{D} = \begin{cases} g(\beta,D)\dot{\beta}, & \text{if } \beta\geqslant 0,\ \dot{\beta}\geqslant 0, \\ 0, & \text{otherwise}, \end{cases} \tag{5}$$

with $D(0) = 0$, where g is a damage rule function. The function $t \mapsto g(\beta(t),D(t))$ is assumed to be increasing when the fundamental postulate holds. Usually D is normalized such that the failure happens at the time moment T_f where $D(T_f) = 1$. The original choice of Ottosen et al. [14] is the damage rule of the exponential form

$$g(\beta,D) = K\exp(L\beta), \tag{6}$$

where K and L are positive material parameters. This damage rule does not depend on D, and hence it does not depend on damage evolution history. We call it the OSR damage rule.

The first natural problem is to estimate the parameters of the model $\boldsymbol{\theta} = (A,\sigma_{-1},C,K,L)$ from the measured Wöhler curves of a material. The complete algorithm is given by Ottosen et al. [14], and it is tested with the experimentally measured data.

3. Accumulated damage rule of Lemaitre and Chaboche

In this paper, we study the damage rule given by Lemaitre and Chaboche, cf. [8,7], of the form

$$g\left(\beta,D\right) = \frac{K}{(1-D)^{\gamma}}\exp\left(L\beta\right), \tag{7}$$

where γ is a new positive parameter of the model. This damage rule is called accumulated, since the damage history depends on the state of the damage *i.e.* the function g depends on D. It is called the LC damage rule and the corresponding model is the LC model.

Remark 3.1. If the damage rule is separable, *i.e.* $g(\beta,D) = g_1^{-1}(D)g_2(\beta)$, then a change of the damage variable yields the OSR model, cf. [8,9,27]. In fact, let $G(D)$ be a primitive of $g_1(D)$, *i.e.* $G'(D) = g_1(D)$, and denote $D_1 = G(D)$. Substituting these equations into the damage evolution Eq. (5) gives us the OSR damage evolution equation $\dot{D_1} = g_2(\beta)\dot{\beta}$.

Note that in our case, the new damage variable D_1 contains the parameter γ. If we know its value, then we may compute parameter estimates C,K and L by Procedure 1 below. Otherwise, we have to estimate γ from experimental data, as explained in Section 5. Finally $D = G^{-1}(D_1)$.

Since we do not change the form of β, the estimation of σ_{-1} and A is the same as the original case in [14]. They are obtained from the linear part of the Haigh diagram given by the equation

$$\sigma_a + A\sigma_m - \sigma_{-1} = 0. \tag{8}$$

Hence σ_{-1} is the fatigue limit for $\sigma_m = 0$ and A is the negative of the slope of the line.

With C,K,L and γ, we proceed as follows. Assume that we have an experimental dataset $(\sigma_a^{(i)},\sigma_m^{(i)},N_{\exp}^{(i)}), i = 1,\ldots,n$, where the fatigue failure takes place at the $N_{\exp}^{(i)}$th cycle. Assume further that the uniaxial stress loading $\sigma(t) = \sigma_m + \sigma_a\sin(t)$ is applied. It follows that the stress varies periodically between $\sigma_2 = \sigma_m + \sigma_a$ and $\sigma_4 = \sigma_m - \sigma_a$.

At stress state σ_1, the load path crosses the endurance surface. When the load increases from state σ_1 to state σ_2, then $\beta > 0$ and $\dot{\beta} > 0$. Hence, the damage increases. When the stress decreases from state σ_2, the damage remains constant until at state σ_3 it reaches the endurance surface and $\beta > 0$ and $\dot{\beta} > 0$, when state σ_3 decreases to state σ_4. Let α_i be the backstress at the state σ_i for $i = 1,2,3,4$. Now $\alpha_1 = \alpha_4, \alpha_2 = \alpha_3$ and Ottosen et al. [14] show that the positions of endurance surface α_2 and α_4 are given by the equations

$$\begin{cases} \frac{3}{2}\alpha_2 - \left(A+1\right)\sigma_2 + \sigma_{-1} - \frac{\sigma_{-1}}{CA}\left(A+1\right)\ln\left(\dfrac{1-\frac{CA}{\sigma_{-1}}\left(\sigma_2 - \frac{3}{2}\alpha_2\right)}{1-\frac{CA}{\sigma_{-1}(A+1)}\left(\sigma_{-1} - \frac{3}{2}A\alpha_4\right)}\right) = 0 \\ -\frac{3}{2}\alpha_4 - \left(A-1\right)\sigma_4 + \sigma_{-1} - \frac{\sigma_{-1}}{CA}\left(A-1\right)\ln\left(\dfrac{1-\frac{CA}{\sigma_{-1}}\left(\sigma_4 - \frac{3}{2}\alpha_4\right)}{1-\frac{CA}{\sigma_{-1}(A-1)}\left(\sigma_{-1} - \frac{3}{2}A\alpha_2\right)}\right) = 0. \end{cases} \tag{9}$$

Since for uniaxial case, the stress tensor $\boldsymbol{\sigma}$ and the backstress tensor $\boldsymbol{\alpha}$ are defined as

$$\boldsymbol{\sigma} = \begin{bmatrix} \sigma & 0 & 0 \\ 0 & 0 & 0 \\ 0 & 0 & 0 \end{bmatrix} \quad \text{and} \quad \boldsymbol{\alpha} = \begin{bmatrix} \alpha & 0 & 0 \\ 0 & -\frac{\alpha}{2} & 0 \\ 0 & 0 & -\frac{\alpha}{2} \end{bmatrix}, \tag{10}$$

then a straightforward matrix computation shows that

$$\beta = \frac{1}{\sigma_{-1}}\left(|\sigma - \frac{3}{2}\alpha| + A\sigma - \sigma_{-1}\right). \tag{11}$$

Now suppose that we are dealing with the jth cycle. Integrating the damage evolution equation

$$(1 - D(t))^{\gamma}\dot{D}\left(t\right) = \begin{cases} K\dot{\beta}(t)\exp(L\beta(t)), & \text{if } \beta\geqslant 0,\ \dot{\beta}\geqslant 0, \\ 0, & \text{otherwise}, \end{cases} \tag{12}$$

from σ_1 to σ_2 and from σ_3 to σ_4 respectively we obtain

$$-\frac{1}{\gamma+1}\left(1 - D_2^{(j)}\right)^{\gamma+1} + \frac{1}{\gamma+1}\left(1 - D_1^{(j)}\right)^{\gamma+1} = \frac{K}{L}(\exp(L\beta_2) - 1) \tag{13}$$

and

$$-\frac{1}{\gamma+1}\left(1 - D_4^{(j)}\right)^{\gamma+1} + \frac{1}{k+1}\left(1 - D_3^{(j)}\right)^{\gamma+1} = \frac{K}{L}(\exp(L\beta_4) - 1). \tag{14}$$

Since damage does not accumulate from σ_2 to σ_3, then $D_3^{(j)} = D_2^{(j)}$. Adding these equations yields

$$-\frac{1}{\gamma+1}\left(1 - D_4^{(j)}\right)^{\gamma+1} + \frac{1}{\gamma+1}\left(1 - D_1^{(j)}\right)^{\gamma+1} = \frac{K}{L}(\exp(L\beta_2) + \exp(L\beta_4) - 2). \tag{15}$$

Note that $a = \frac{K}{L}(\exp(L\beta_2) + \exp(L\beta_4) - 2)$ is constant over the cycles.

Denoting $u_j = \frac{1}{\gamma+1}\left(1 - D_1^{(j)}\right)^{\gamma+1}$ and taking into account that $D_4^{(j)} = D_1^{(j+1)}$, we obtain a difference equation

$$u_{j+1} - u_j = -a,\ u_1 = \frac{1}{\gamma+1},\ j = 1, 2, \cdots. \tag{16}$$

$$\int_0^{T_f} K\left(\gamma\right)\dot{\beta}\exp\left(L\beta\right)H\left(\beta\right)H\left(\dot{\beta}\right)\,dt = \frac{1}{\gamma+1}\int_0^{T_f} K\left(0\right)\dot{\beta}\exp\left(L\beta\right)H\left(\beta\right)H\left(\dot{\beta}\right)\,dt = \frac{1}{\gamma+1} \tag{21}$$

It is easy to see, cf. [20], that the solution to this equation is given by

$$u_j = \frac{1}{\gamma+1} - \left(j-1\right)a,\ j = 1, 2, \cdots. \tag{17}$$

Now if it takes $N(\gamma)$ cycles to damage failure, then $1 = D_4^{(N(\gamma))} = D_1^{(N(\gamma)+1)}$. It follows that $0 = u_{N+1} = \frac{1}{\gamma+1} - Na$ and hence

$$\frac{1}{N(\gamma)} = \left(\gamma+1\right)a = \frac{(\gamma+1)K}{L}(\exp(L\beta_2) + \exp(L\beta_4) - 2). \tag{18}$$

Note that when $\gamma = 0$, this result is in agreement with the number of cycles given by Ottosen et al. [14].

Theorem 3.1. *In the LC model, the parameters γ and K are not identifiable.*

Proof. Let $K(\gamma)$ be the optimal parameter K in the LC model. Hence $K(0)$ is the optimal parameter K in the OSR model, which does not contain γ at all.

Now let us fix $\gamma > 0$. Comparing the Eq. (18) with parameters $\gamma > 0$ and $\gamma = 0$, we see that $(\gamma+1)K$ gives at the optimum point the same residual sum of squares as the OSR model. Hence γ and $K(\gamma)$ are optimal parameters for the LC model. But $(\gamma+1)K(\gamma) = K(0)$.

It follows that for all $\gamma > 0$ we have $K(\gamma) = K(0)/(\gamma+1)$ and γ are optimal for the LC model, which completes the proof. □

We see that parameters γ and K are related by $(\gamma+1)K = w$, where w is a constant, giving the same amount of cycles for uniaxial periodic stress histories with a constant amplitude. Surprisingly, this result holds true for any kind of stress history.

Theorem 3.2. *For any parameter $\gamma\geqslant 0$, the OSR model with parameter $K(0)$ and the LC model with parameter $K(\gamma) = K(0)/(\gamma+1)$ give the same lifetime with all stress histories.*

Proof. For $\gamma\geqslant 0$, let D_γ denote the fatigue accumulation function. Now the damage evolution Eq. (12) can be written compactly as

$$(1 - D_\gamma)^{\gamma}\dot{D}_\gamma = K\dot{\beta}\exp\left(L\beta\right)H\left(\beta\right)H\left(\dot{\beta}\right), \tag{19}$$

where H is the Heaviside function.

We first consider the case $\gamma = 0$, *i.e.* the OSR damage rule. Suppose that we have estimated the parameters of the model. Now run the model with an arbitrary stress loading $\sigma(t)$ and obtain a lifetime T_f. Integrating the Eq. (19) over the interval $[0\ T_f]$ and using the boundary values $D_0(0) = 0$ and $D_0(T_f) = 1$, we get

$$\begin{aligned} 1 = D_0\left(T_f\right) - D_0\left(0\right) &= \int_0^{T_f} \dot{D}_0\,dt \\ &= \int_0^{T_f} K\left(0\right)\dot{\beta}\exp\left(L\beta\right)H\left(\beta\right)H\left(\dot{\beta}\right)\,dt. \end{aligned} \tag{20}$$

Next, take $\gamma > 0$ and a new parameter $K(\gamma) = K(0)/(\gamma+1)$. The other model parameters remain unchanged. As before we run the modified model with the same stress loading $\sigma(t)$. Note that since we change only the parameters of the fatigue evolution equation, we get the same $\beta(t)$ as with the OSR damage rule. Now we integrate the Eq. (19) over $[0, T_f]$, where T_f is the lifetime obtained with the OSR damage rule. The right-hand side of the Eq. (19), using the result of (20), yields (21), and the left-hand side gives

$$\frac{1}{\gamma+1}\left((1 - D_\gamma(0))^{\gamma+1} - \left(1 - D_\gamma(T_f)\right)^{\gamma+1}\right).$$

Since $D_\gamma(0) = 0$, we get $1 - (1 - D_\gamma(T_f))^{\gamma+1} = 1$ and consequently $(1 - D_\gamma(T_f))^{\gamma+1} = 0$. Hence $D_\gamma(T_f) = 1$, which completes the proof. □

We emphasize that by Theorem 3.1 it is not possible to estimate both parameters K and γ based only on the measured values of a Wöhler curve. Similarly, Theorem 3.2 tells us, that preceding parameters are not estimable with any multiaxial fatigue data. In Section 5, we will discuss the possibility to estimate the parameter γ with some additional experimental data. However we may compute the optimal parameters for the LC model with $\gamma > 0$ from the optimal parameters of the OSR model with the OSR damage rule as given in the proof in Theorem 3.1.

Now let $\gamma\geqslant 0$ be fixed. Hence, we may find the corresponding parameters, similarly as in [14], by minimizing the sum of squares

$$S\left(C,K,L\right)=\sum_{i=1}^{n}\left(\ln N_{\exp}^{(i)}-\ln N^{(i)}\left(\gamma\right)\right)^{2}, \tag{22}$$

where $N^{(i)}$ is the predicted number of cycles given by (18) and $N_{\exp}^{(i)}$ is the experimentally obtained number of cycles.

For physical reasons, the true model parameters are positive. Since the terms $1/N^{(i)}$ are small, then some iterates may give a negative value for some terms, resulting in a complex value for $\ln N^{(i)}$. It follows that the algorithm fails to give a correct result.

For these reasons, we have to minimize $S(C,K,L)$ subject to the constraints $C\geqslant 0,\ K\geqslant 0,\ L\geqslant 0$, which is a classical nonlinear regression problem. These problems are discussed extensively by Seber and Wild [22]. The state-of-the-art algorithm for the bounded variable nonlinear least squares problem is the reflective trust region method. For more information on this algorithm, see Coleman and Li [5].

3.1. *Estimation of parameters C, K and L*

By the previous results, the following procedure gives an estimate for $C,\ K$ and L.

- **Procedure 1**, which calibrates model parameters $C,\ K$ and L.
1. Fix $\gamma\geqslant 0$, $\gamma=0$ as default value.
2. Initialize the parameters.
3. Iterate the following steps:
a. For $i=1,\ldots,n$ do
   - Input $(\sigma_a^{(i)},\sigma_m^{(i)},N_{\exp}^{(i)})$.
   - Set $\sigma_2=\sigma_m^{(i)}+\sigma_a^{(i)}$ and $\sigma_4=\sigma_m^{(i)}-\sigma_a^{(i)}$.
   - Solve (9) for (α_2,α_4).
     Note that there is no analytic solution of (9). Hence a numerical solution of the system is computed.
   - Compute $N^{(i)}(\gamma)$ by (18).
   - Set $b_i=\left(\ln N_{\exp}^{(i)}-\ln N^{(i)}\right)$.
b. Evaluate the object function $S(C,K,L,\gamma)=\sum_{i=1}^{n}b_i^2$.
c. Update the parameters.
d. Stop iteration when a termination criterion takes effect.

4. Comparison with experimental data

We have three different datasets. Measurements of alloy steel SAE 4340 were adopted from [14]. In addition, we used measurements of alloy steel SAE 7475 and aluminium alloy SAE 6156. Table 1 gives the model parameter estimates obtained with these datasets.

Since the target function S around the optimum point is flat, the numerical solution of the problem is difficult. We observed that from different initial points, the optimizer converged to different solutions. Hence, we selected a grid of initial values and accepted as optimum the solution with the smallest sum of squares.

It is well known that the Wöhler curve of a ferrous alloy and titanium shows a clear fatigue limit, *i.e.* the curve looks like a hockey stick. Instead the Wöhler curve of a nonferrous alloy, excluding titanium, decreases smoothly without a sharp bend. Figs. 1 and 2 demonstrate this fact.

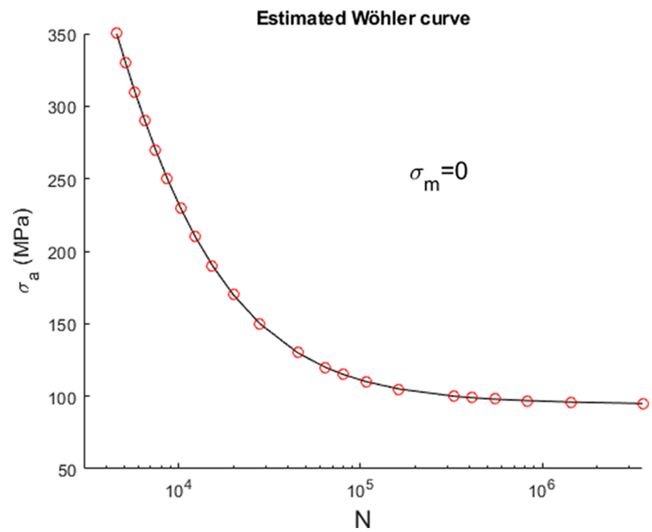

Fig. 1. Wöhler curve of CoCrNi alloy steel SAE 7475.

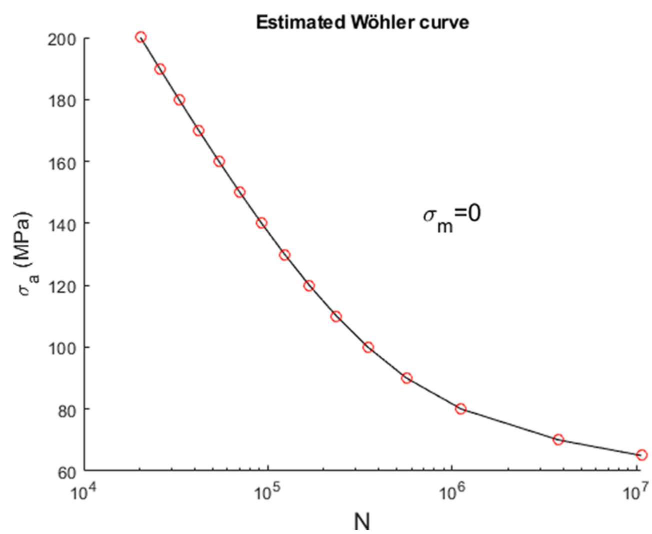

Fig. 2. Wöhler curve of aluminium alloy SAE 6156.

5. Estimating the parameter γ

As we saw above, it is not possible to estimate γ from Wöhler data. We need additional information on the development of fatigue damage. Recently new measurement techniques have been introduced, as mentioned in the Introduction. In this paper we use the results of [23].

By the estimation methods described above, we can estimate model parameters, and as we saw, we can choose $\gamma\geqslant 0$ such that $(\gamma+1)K=w$. To obtain a value for γ, we first show how the fatigue develops. Let n denote the cycle index and $N(\gamma)$, as before, the lifetime. As discussed above, $N(\gamma)$ is the same for all γ. Denote by N_f the shared value and $x=\frac{n}{N_f}$.

Theorem 5.1. *For all $\gamma\geqslant 0$*

Table 1
Parameters of the OSR model for some materials.

Material	#Obs	A	σ_{-1}	C	K	L	SSQ
NiCrMo alloy steel SAE 4340	20	0.2250	490	0.8083	6.9668e-06	18.4562	10.4044
Aluminium alloy SAE 6156	42	1.2000	75	0.8883	1.8557e-06	0.9140	16.4712
CoCrNi alloy steel SAE 7475	36	0.3571	95	1.1000	3.8126e-05	0.2007	1172.6

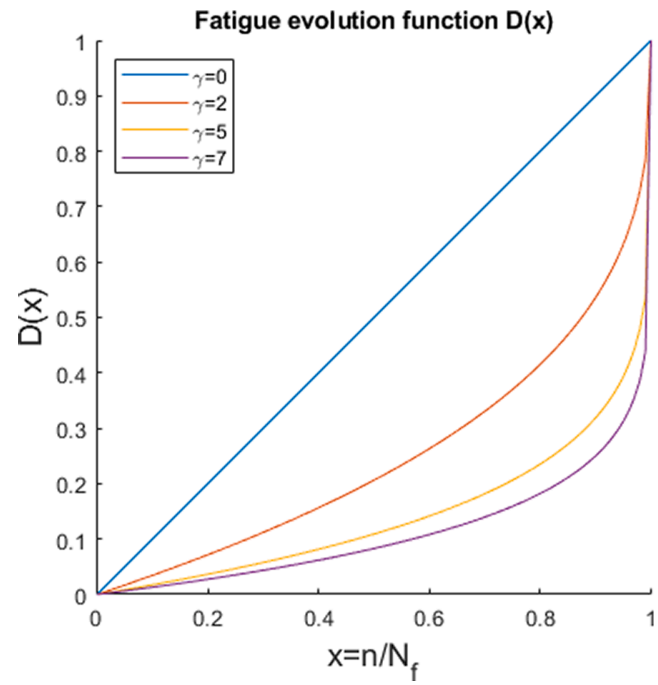

Fig. 3. Failure evolution functions D.

$$D(x) = 1-(1-x)^{\frac{1}{\gamma+1}},\ 0\leqslant x\leqslant 1. \tag{23}$$

Proof. Let

$$h(u) = -\frac{1}{\gamma+1}(1-u)^{\gamma+1},\ 0\leqslant u\leqslant 1. \tag{24}$$

Then direct computation gives

$$h^{-1}(v) = 1-(-(\gamma+1)v)^{\frac{1}{\gamma+1}},\ -\frac{1}{\gamma+1}\leqslant v\leqslant 0. \tag{25}$$

Now by Eq. (15), we see that the increase of $h \circ D$ is constant over cycles. Hence $h(D(x))$ is a straight line from $(0, h(D(0)))$ to $(1, h(D(1)))$. Since $D(0) = 0$ and $D(1) = 1$, then

$$h\left(D\left(x\right)\right) = h\left(0\right) + \left(h\left(1\right)-h\left(0\right)\right)x = -\frac{1}{\gamma+1}\left(1-x\right) \tag{26}$$

and hence

$$D(x) = h^{-1}\left(-\frac{1}{\gamma+1}\left(1-x\right)\right) = 1-(1-x)^{\frac{1}{\gamma+1}}. \tag{27}$$

□ Some fatigue evolution functions $D(x)$ are illustrated in Fig. 3.

Suppose we have observations (x_i, d_i), $i = 1, \ldots, p$ of the fatigue development. We choose such a parameter γ, which minimizes the sum of squares

$$g(\gamma) = \sum_{i=1}^{p}(d_i - D(x_i))^2. \tag{28}$$

Since the derivatives $g'(\gamma)$ and $g''(\gamma)$ are easily calculated, then the Newton method gives the optimal γ in a few iterations.

The values of damage variable D can be obtained by measuring the static relative ductility change of a material, see [23], or by measuring the electrical resistance of structural steel, see [25].

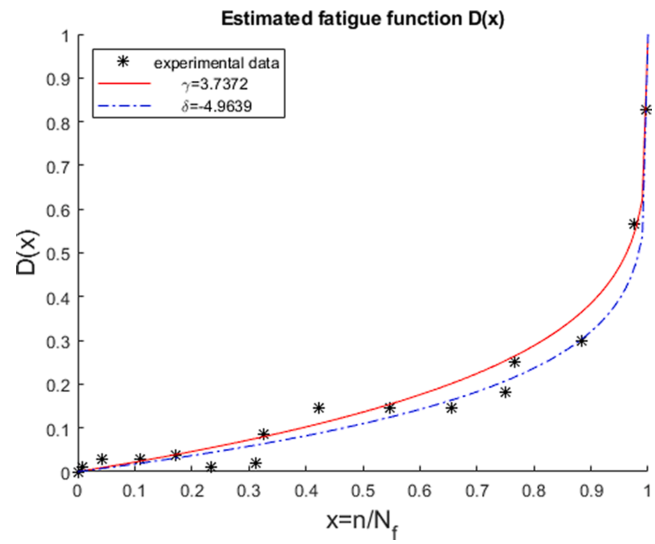

Fig. 4. Failure evolution functions D with one dataset.

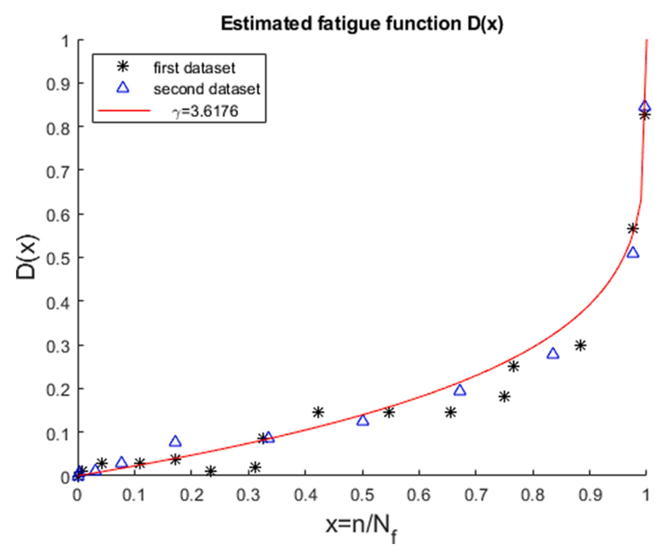

Fig. 5. Failure evolution function D with the combined dataset.

Shang and Yao [23] developed a model for damage accumulation from a different point of view. They derived a cumulative fatigue function, which in our notation reads

$$D = 1-\left(1-\frac{n}{N_f}\right)^{\frac{1}{1-\delta}}, \tag{29}$$

where

$$\delta\left(\sigma_a, \sigma_m\right) = 1-\frac{H\left(\sigma_a-\sigma_{fl}\left(\sigma_m\right)\right)}{a\ln\left(\left|\sigma_a-\sigma_{fl}\left(\sigma_m\right)\right|\right)}. \tag{30}$$

Here H is the Heaviside function, a is a material parameter, which can be

Table 2
Parameters of the LC model for 20 Mn structural steel.

Material	γ	A	σ_{-1}	C	K	L
20 Mn steel	7.3533	0.3214	740	4.3078e-4	1.0802e-6	5.1690

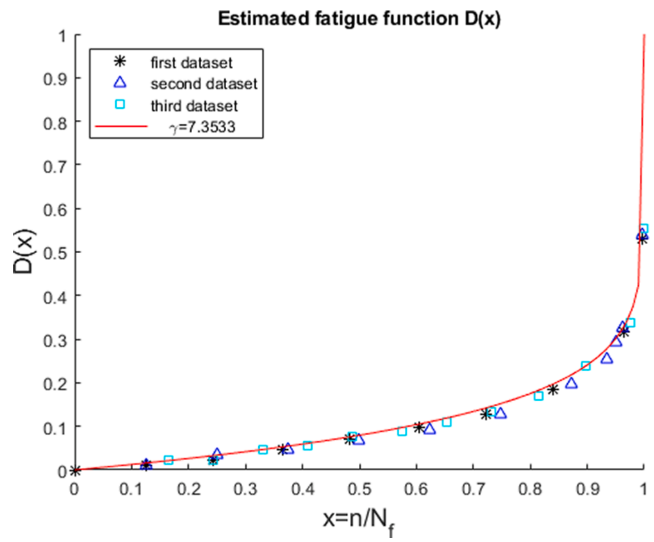

Fig. 6. Fatigue accumulation curve for 20 Mn steel.

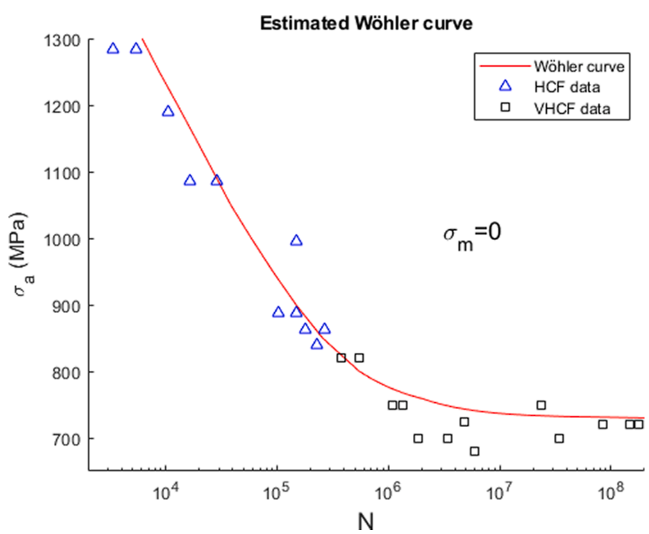

Fig. 7. Wöhler curve of 20 Mn steel.

estimated, and $\sigma_{fl}(\sigma_m) = \sigma_{-1} - A\sigma_m$ denotes the fatigue limit when the mean stress σ_m is applied.

If we denote $\gamma = -\delta$, then the LC model and Shang–Yao model appear to be the same. However, in the LC model, γ is a model parameter, which is assumed to be valid for all kinds of stress histories. In the Shang–Yao model, as given in the Eq. (30), δ depends on the amplitude and mean stress of the applied stress loading.

As an example, we use the measurements of Shang and Yao for 16 Mn steel in Figs. 2(a) and 2(b) in [23]. First, we take only the data in Fig. 2 (a). Now the least squares estimation gives $\gamma = 3.7372$. With the information given in [23], we are able to compute $\delta = -4.9639$. The resulting failure functions are given in Fig. 4.

Next we combine the data from the figures and obtain $\gamma = 3.6176$. Since the datasets are measured with a different amplitude, we are not able to compute δ at all. Fig. 5 illustrates the situation.

Finally, we apply the model to 20 Mn structural steel. The computed parameter estimates are given in Table 2.

Parameter γ was estimated from the measured fatigue profiles provided by Sun et al. [25]. The estimated fatigue accumulation is depicted in Fig. 6.

For the estimation of C, K and L, we used data on the high-cycle fatigue (HCF) domain given in [6]. Data for A and σ_{-1} were obtained from [3]. Fig. 7 gives the estimated Wöhler curve.

In Fig. 7, we also plot the HCF data used in parameter estimation. In addition, measurements done in the very-high-cycle fatigue (VHCF) domain are plotted. These data are given in [3]. We see that the model fits nicely with the data in the HCF domain. However, in the VHCF domain, the observations are mostly below the values predicted by the LC model. Note that the LC model was developed for the HCF domain. The observed gap indicates that for the VHCF domain, a new model is needed [15]. Recall that some physical processes causing fatigue failure may behave differently in the HCF and VHCF domain [11,15,21].

5.1. Case example

Suppose that we have estimated all the parameters of the model. Now we will apply a uniaxial periodic stress loading. The problem is how many cycles N_p it will take until the damage function D attains a value $p \in (0, 1)$. By Theorem 5.1, we have to solve the equation $p = D(x) = 1 - (1 - x)^{\frac{1}{\gamma+1}}$ for x, which gives $x = 1 - (1 - p)^{\gamma+1}$. It follows that $N_p = xN_f$.

Suppose we have a specimen of 20 Mn steel and we apply a sinusoidal stress with $\sigma_m = 0$ and $\sigma_a = 750$ MPa. Now we are interested in how many cycles it will take to reach 50% of the lifetime. The Wöhler curve in Fig. 7 gives $N_f = 3061474$. Hence $N = xN_f = 3052113$.

6. Conclusions

The parameter determination of the OSR model for high-cycle fatigue with the Lemaitre-Chabouche type damage rule is proposed. Let $K(0)$ be the optimal K-parameter for the OSR model. We proved that all parameters K and γ satisfying the equation $(\gamma + 1)K = K(0)$ give the same residual sum of squares as $K = K(0)$ and $\gamma = 0$. It follows that these parameters are not estimable from observations of the Wöhler curve (or more generally, not from multiaxial fatigue data) only. Furthermore, it is shown that with experimental data from the fatigue development profile, it is possible to estimate γ and consequently K.

Hence, the LC model provided an explicit function for the fatigue development profile. Shang and Yao [23] introduced a similar function. However, the parameter δ of the Shang–Yao model depends on the mean stress and amplitude of the stress loading. If the experimental data contain measurements with a different mean stress or amplitude, then it is impossible to compute a value of δ at all. Furthermore, the application of the model demands, except a value for δ, information about what kind of data the computation of δ was based on. In the computation of the γ-parameter of the LC model, it is possible, and even advantageous, to use all the data, which gives a more reliable estimate.

We also observed that the LC model fits well with observations in the HCF domain. The discrepancy in the VHCF domain suggests that a new model is needed in that domain.

Declaration of Competing Interest

The authors declare that they have no known competing financial interests or personal relationships that could have appeared to influence the work reported in this paper.

Acknowledgements

Authors wish to thank Prof. Dr. Jürgen Bár (Universität der Bundeswehr Múnchen) for delivering the measurement data of the alloy steel SAE 7475 and the aluminium alloy SAE 6156 used in Section 4, MSc. Joonas Lahtinen (Tampere University) for the routine numerical calculations to give us a better understanding of the role of γ in the model and Prof. Ilya Keller (Institute of Continuous Media Mechanics UB RAS, Perm) for the valuable suggestions and exchange of ideas.

Appendix A. Supplementary material

Supplementary data associated with this article can be found, in the online version, at https://doi.org/10.1016/j.ijfatigue.2021.106153.

References

[1] Aeran A, Siriwardane S, Mikkelsen O, Langen I. A new nonlinear fatigue damage model based only on S-N curve parameters. Int J Fatigue 2017;103:327–41.
[2] Aeran A, Siriwardane S, Mikkelsen O, Langen I. An accurate fatigue damage model for welded joints subjected to variable amplitude loading. IOP Conf Series: Mater Sci Eng 2017;276:12–38.
[3] Burkart K, Bomas H, Zoch H-W. Fatigue of notched case-hardened specimens of steel SAE 5120 in the VHCF regime and application of the weakest-link concept. Int J Fatigue 2011;33:59–68.
[4] Chaboche JL. Lifetime predictions and cumulative damage under high-temperature conditions. In: Amzallag C, Leis B, Rabbe P, editors. Low-cycle fatigue and life prediction. West Conshohocken, PA: ASTM International; 1982. p. 81–104.
[5] Coleman TF, Li Y. An interior trust region approach for nonlinear minimization subject to bounds. SIAM J Optim 1996;6:418–45.
[6] Dengo C, Meneghetti G, Dabalà M. Experimental Analysis of Bending Fatigue Strength of Plain and Notched Case-Hardened Gear Steels. Int J Fatigue 2015;80: 145–61.
[7] Holopainen S, Kouhia R, Saksala T. Continuum approach for modeling transversely isotropic high-cycle fatigue. Eur J Mech A/Solids 2016;60:183–95.
[8] Lemaitre J, Chaboche JL. Mechanics of solid materials. Cambridge University Press; 1990.
[9] Lindström SB. Continuous-time, high-cycle fatigue model for nonproportional stress with validation for 7075–T6 aluminum alloy. Int J Fatigue 2020;140. https://doi.org/10.1016/j.ijfatigue.2020.105839.
[10] Lindström SB, Thore C, Suresh S, Klarbring A. Continuous-time, high-cycle fatigue model: Validity range and computational acceleration for cyclic stress. Int J Fatigue 2020;136. https://doi.org/10.1016/j.ijfatigue.2020.105582.
[11] Marines I, Bin X, Bathias C. An understanding of very high cycle fatigue of metals. Int J Fatigue 2003;25:1101–7.
[12] Miner MA. Cumulative damage in fatigue. J Appl Mech 1945;12:159–64.
[13] Ottosen N, Ristinmaa M, Kouhia R. Enhanced multiaxial fatigue criterion that considers stress gradient effects. Int J Fatigue 2018;116:128–39.
[14] Ottosen N, Stenström R, Ristinmaa M. Continuum approach to high-cycle fatigue modeling. Int J Fatigue 2008;30:996–1006.
[15] Paolino DS, Tridello A, Geng HS, Chiandussi G, Rossetto M. Duplex S-N fatigue curves: statistical distribution of the transition fatigue life. Frattura ed Integrità Strutturale 2014;30:417–23. https://doi.org/10.3221/IGF-ESIS.30.50.
[16] Pavlou DG. The influence of the crack tip plastic zone strain hardening on the metal High-Cycle-Fatigue behavior. In: Proceedings of the Fifth International Conference of Structures under Shock and Impact-1998. Thessaloniki, Southampton: WIT Press; 1998. p. 633–47.
[17] Pavlou DG. Prediction of fatigue crack growth under real stress histories. Eng Struct 2000;22:1707–13.
[18] Pavlou DG. A phenomenological fatigue damage accumulation rule based on hardness increasing, for the 2024–T42 aluminum. Eng Struct 2002;24:1363–8.
[19] Plumtree A, Nilson J-O. High temperature fatigue damage in three austenitic alloys, Fatigue & Fracture of Engineering. Mater Struct 1988;11:397–407.
[20] Råde L, Westergren B. Mathematics Handbook for Science and Engineering, Studentlitteratur, 1995.
[21] Sadek M, Bergström J, Hallbäck N, Burman C, Elvira R, Escauriaza B. Fatigue strength and fracture mechanisms in the very-high-cycle-fatigue regime of automotive steels. Steel Res Int 2020;91. https://doi.org/10.1002/srin.202000060.
[22] Seber GAF, Wild CJ. Nonlinear regression. Wiley; 2003.
[23] Shang D-Q, Yao W-X. A nonlinear cumulative model for uniaxial fatigue. Int J Fatigue 1999;21:187–94.
[24] Sih G-C, Jeong D-Y. Fatigue load sequence effect ranked by critical available energy density. Theoret Appl Fract Mech 1990;14:1–11.
[25] Sun B, Yang L, Guo Y. A high-cycle fatigue accumulation model based on electrical resistance for structural steels. Fatigue Fracture Eng Mater Struct 2007;30: 1052–62. https://doi.org/10.1111/j.1460-2695.2007.01175.x.
[26] Suresh S. Fatigue of materials. Cambridge University Press; 1998.
[27] Suresh S, Lindström SB, Thore C, Torstenfelt B, Klarbring A. Topology optimization using a continuous-time high-cycle fatigue model. Struct Multidisc Optim 2020;61: 1011–25. https://doi.org/10.1007/s00158-019-02400-w.